

# MonkeyOCR: Document Parsing with a Structure-Recognition-Relation Triplet Paradigm

Zhang Li<sup>1</sup>, Yuliang Liu<sup>1,†</sup>, Qiang Liu<sup>2</sup>, Zhiyin Ma<sup>1</sup>, Ziyang Zhang<sup>1</sup>,  
 Shuo Zhang<sup>1</sup>, Biao Yang<sup>1</sup>, Zidun Guo<sup>1</sup>, Jiarui Zhang<sup>2</sup>, Xinyu Wang<sup>1</sup>, Xiang Bai<sup>1</sup>  
<sup>1</sup>Huazhong University of Science and Technology, <sup>2</sup>Kingsoft Office  
 † Project lead

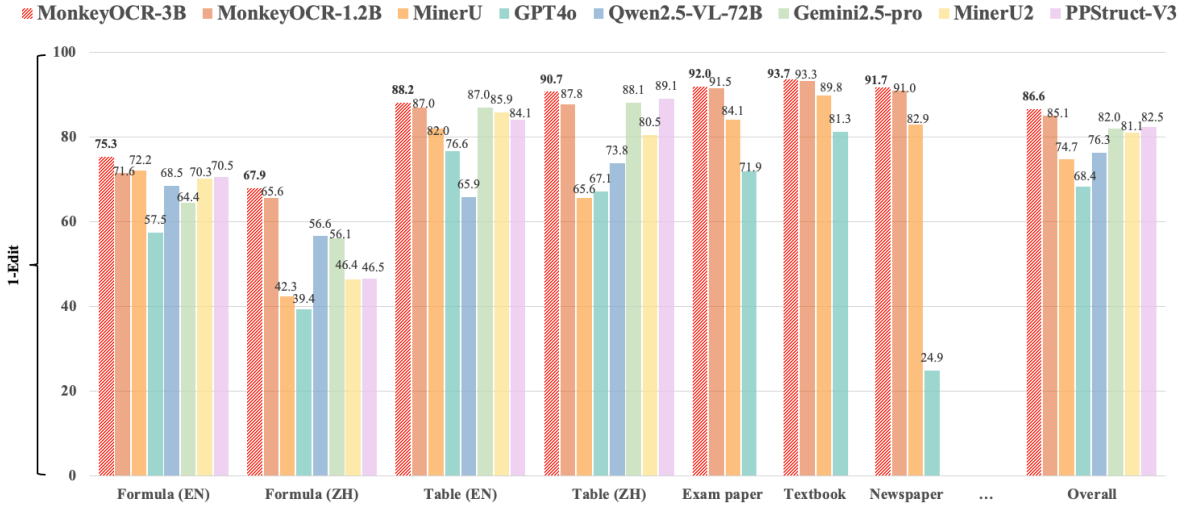


Figure 1. Performance comparison of MonkeyOCR and other SOTA models on OmniDocBench [37].

## Abstract

We introduce *MonkeyOCR*, a document parsing model that advances the state of the art by leveraging a *Structure-Recognition-Relation (SRR) triplet paradigm*. This design simplifies what would otherwise be a complex multi-tool pipeline and avoids the inefficiencies of processing full pages with giant end-to-end models. In SRR, document parsing is abstracted into three fundamental questions — “Where is it?” (structure), “What is it?” (recognition), and “How is it organized?” (relation) — corresponding to structure detection, content recognition, and relation prediction. To support this paradigm, we present *MonkeyDoc*, a comprehensive dataset with 4.5 million bilingual instances spanning over ten document types, which addresses the limitations of existing datasets that often focus on a single task, language, or document type. Leveraging the SRR paradigm and *MonkeyDoc*, we trained a 3B-parameter document foundation model. We further identify parameter redundancy in this model and propose *contiguous parameter degradation (CPD)*, enabling the construction of models from 0.6B to 1.2B parameters that run faster with ac-

ceptable performance drop. *MonkeyOCR* achieves state-of-the-art performance, surpassing previous open-source and closed-source methods, including Gemini 2.5-Pro. Additionally, the model can be efficiently deployed for inference on a single RTX 3090 GPU. Code and models will be released at <https://github.com/Yuliang-Liu/MonkeyOCR>.

## 1. Introduction

Document parsing aims to systematically convert the complex multimodal content (including texts, tables, images, formulas, etc.) within various documents (such as scanned images and PDF files) into structured information. This technology has a wide range of applications, including smart office solutions, intelligent education systems, digitization of medical records and judicial documents, and the preservation of historical documents.

Recent mainstream document parsing methods can be broadly categorized into pipeline-based toolchains and end-to-end models. Pipeline-based toolchains, such as

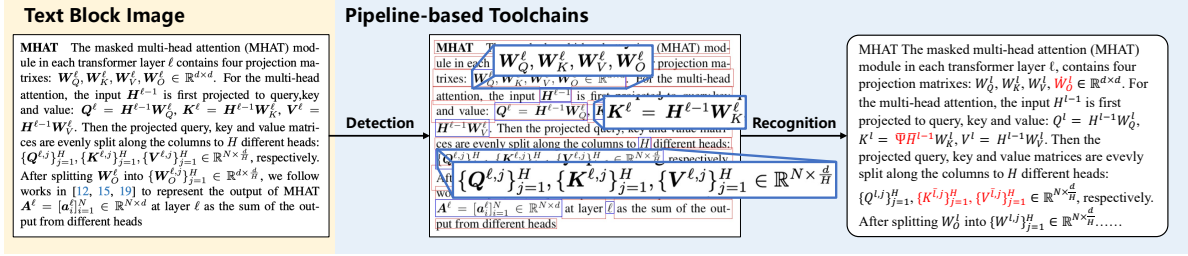


Figure 2. A typical example of cumulative error in pipeline-based toolchains.

MinerU [49] and PPStruct-V3 [9], break down the complex parsing task into fine-grained sub-tasks, with each sub-task handled by specialized models. This modular approach allows each component to be optimized independently. In contrast, giant end-to-end models [1] directly inputting entire document page images into a unified model for holistic content recognition, resulting in a streamlined workflow.

Although existing document parsing approaches have achieved remarkable progress, they still suffer from inherent limitations. First, pipeline-based methods suffer from cumulative error caused by the combination of multiple fine-grained tools. These methods typically follow a sequential process: layout detection, text and formula detection, instance-level recognition, element merging, and finally reading order reconstruction. As shown in Fig. 2, imprecise formula detection results in partial cropping of characters from the previous line, leading to erroneous recognition outcomes, such as the inclusion of extraneous superscripts. Second, end-to-end models often face limitations in both performance and efficiency when dealing with lengthy contexts. Document pages are typically of high resolution and contain densely packed information, leading to extremely long input and output sequences. Prior studies [58, 61] have shown that large multimodal models are more prone to hallucinations when processing long contexts. Moreover, the quadratic computational cost of attention makes the processing of long sequences increasingly expensive.

To achieve a balance between accuracy and speed, we propose MonkeyOCR, which adopts a ‘‘Structure-Recognition-Relation’’ (SRR) triplet paradigm for document parsing. Specifically, we first perform structure detection to identify different regions within the document, such as text blocks, tables, formulas, images. Then, to handle multiple recognition tasks with a unified model, we trained a large multimodal model to perform block-level parallel end-to-end recognition of these detected regions. Finally, the coordinate and category of these regions is fed into a block-level reading order prediction model to determine the reading order. Based on the reading order, the results of content recognition are then combined to produce the final document content.

Existing document parsing datasets often focus on a single task (e.g., table recognition or layout analysis), a specific document type (e.g., academic papers), or a single language, which limits the development of robust document parsing models. To address these limitations, we developed a comprehensive data generation pipeline that integrates meticulous manual annotation, programmatic data synthesis, and advanced model-driven automatic labeling, resulting in MonkeyDoc dataset. The dataset contains 4.5 million bilingual instances, covering five document parsing tasks, involving more than ten document types.

Building on the SRR paradigm and the MonkeyDoc dataset, we trained a 3B-parameter document foundation model. We further observed parameter redundancy in this model and, based on experimental findings, empirically propose contiguous parameter degradation (CPD), which continuously skips sequences of intermediate layers to construct lightweight models (0.6B–1.2B parameters) that achieve comparable performance with faster inference. Moreover, our results show that parameter reduction has minimal impact on simple tasks, such as text recognition, but substantially affects more complex tasks, such as table recognition. Compared to pipeline-based methods, MonkeyOCR reduces the cumulative errors caused by multi-tool combination, outperforming the best pipeline method PPStruct-V3 by 4.1%. It also surpasses giant end-to-end model Qwen2.5-VL-72B and the best closed-source model Gemini 2.5-Pro, achieving 2.09× faster inference than the end-to-end baseline. Furthermore, MonkeyOCR-1.2B offers a 34% speed improvement over the 3B model with only a 1.5% performance drop. We summarize the contributions as follows:

- We propose the SRR paradigm, decomposing document parsing into structure detection, content recognition, and relation prediction. This design reduces cumulative errors caused by multi-tool integration and avoids the inefficiencies of processing full pages with end-to-end models.
- We present MonkeyDoc, a comprehensive dataset with 4.5 million bilingual instances covering five document parsing tasks across more than ten document types, addressing the limitations of existing datasets that often fo-

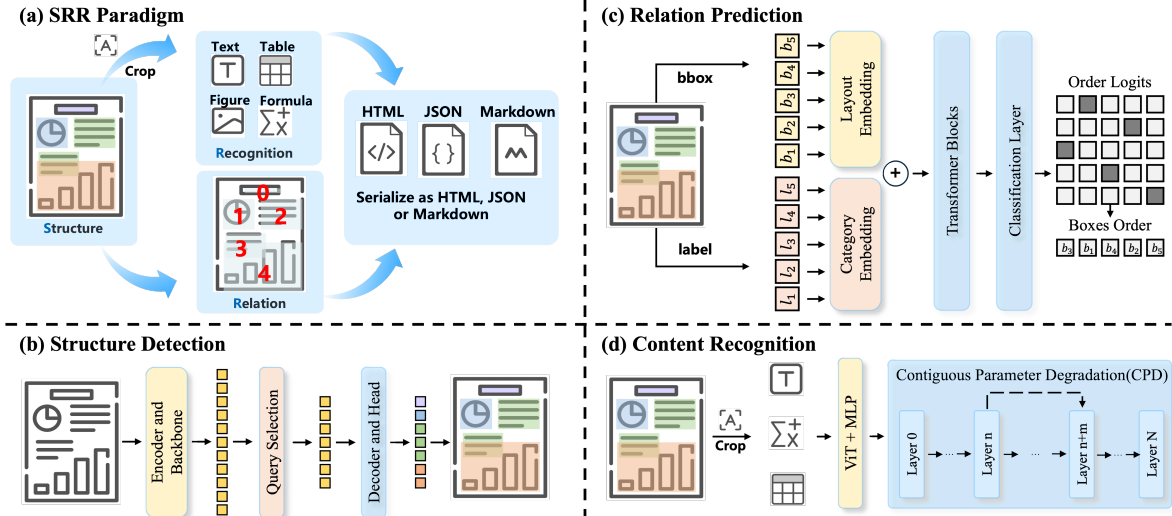


Figure 3. The overall pipeline of MonkeyOCR.

cus on a single task, language, or document type.

- We propose a 3B document foundation model based on the SRR paradigm and MonkeyDoc, and introduce contiguous parameter degradation (CPD) to prune redundant layers. CPD enables the construction of lightweight models (0.6B–1.2B parameters) that achieve comparable performance while offering faster inference.

## 2. Related Work

### 2.1. Pipeline-based Toolchains

Pipeline-based approaches [4, 26, 39, 49] decompose the task of document parsing into multiple sequential steps, such as layout analysis [17, 47, 56], reading order prediction [50], optical character recognition (OCR) [18, 21], formula recognition [48], formula detection, and table recognition [16, 38]. Each step employs a specialized model to handle a specific sub-task. Docling [26] implements a linear processing pipeline to parse PDF files, extract page content (including OCR, layout, and table information), and generate structured documents in JSON or Markdown format. Marker [39] relies on the Surya OCR toolkit [40] for OCR, layout, reading order, and table recognition, with optional LLM modules for cross-page table merging and inline math parsing. Similarly, MinerU and PPstruct-V3 adopt a pipeline of multiple models for layout detection [57], formula detection [19] and recognition [48], OCR [21], table recognition [53, 54], and reading order prediction [15, 50], and integrate these outputs to complete document parsing.

### 2.2. End-to-end Models

End-to-end models streamline document parsing by directly processing full-page images into structured outputs, eliminating the need for multiple task-specific models. Donut [20] introduces the first OCR-free framework for

document understanding, while Nougat [3] adopts a similar architecture to convert document images into Markdown. The SPTS series [24, 41] presents a unified framework for text detection and recognition, and OmniParser [46] extends it to text spotting, key information extraction, and table recognition, enabling robust parsing across both natural scenes and documents. Recently, large multimodal models [1, 6, 23, 25, 51] trained on massive datasets have achieved remarkable progress in end-to-end document understanding. Building on Qwen2.5-VL [1], models such as olmOCR [43], OCRFlux [5], and Nanonets-OCR [28] are further trained on large corpora of PDF pages, enhancing the document parsing capabilities of general-purpose multimodal models. DeepSeekOCR-3B [52] explores visual token compression techniques for efficient document parsing.

### 2.3. Document Parsing Dataset

Document parsing encompasses fine-grained tasks such as layout detection, reading order prediction, and content recognition. A variety of datasets have been developed to support these tasks, each focusing on specific document types, languages or sub-tasks. For layout detection, datasets such as M<sup>6</sup>Doc [7], CDLA [22], D4LA [10], and DocLayNet [42] provide annotations of the positions of structural elements (e.g., text blocks, tables) across diverse document types. For content recognition, table recognition datasets such as FinTabNet [59] and PubTabNet [60] provide large-scale structural and content annotations, while Unimer-1M [48] and HME-100k [55] focus on mathematical expression recognition in printed and handwritten forms. For reading order prediction, ReadingBank [50] provides word-level reading order annotations for 500k documents. Additionally, DocGenome [53] provides annotations for 500K English papers from arXiv, covering major document parsing tasks.

Dataset	Document type	Supporting Tasks					Language	
		Layout Detection	Reading Order Prediction	Formula Recognition	Table Recognition	Text Recognition	EN	ZH
M <sup>6</sup> Doc [7], DocLayNet [42]	6, 2	✓					✓	✓
CDLA [22]	1	✓						✓
D4LA [10]	5	✓					✓	
Unimernet [48], TexTeller [35]	-			✓				
FinTabNet [59], PubTabNet [60]	-				✓			
DocGenome [53]	1	✓	✓	✓	✓	✓	✓	
<b>MonkeyDoc</b>	<b>&gt;10</b>	✓	✓	✓	✓	✓	✓	✓

Table 1. Comparison of MonkeyDoc with other document parsing datasets.

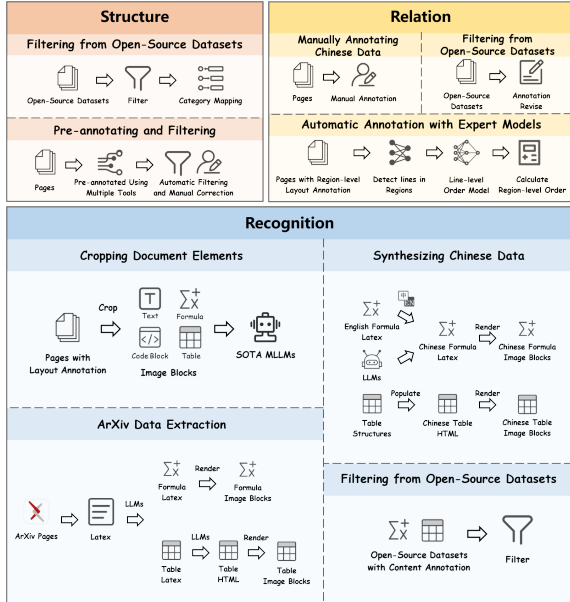


Figure 4. The data generation pipeline of MonkeyDoc.

### 3. MonkeyDoc Dataset

To train MonkeyOCR, we developed a complete data generation pipeline and built a comprehensive document parsing dataset, MonkeyDoc. As shown in Tab. 1, the dataset covers more than ten document types, supports both Chinese and English, and spans the entire document parsing process. The overall data generation pipeline is illustrated in Fig. 4. More details can be found in the appendix.

For structure detection, we collected raw annotations from existing open-source datasets [7, 10, 22, 42, 53], removed nested bounding boxes, and selected samples with richer structural elements to enhance data diversity. Moreover, considering the scarcity of Chinese samples in open-source datasets, we additionally collected over 300k pages Chinese documents, including financial reports, textbooks, academic papers, etc. These pages were pre-annotated using multiple tools [9, 57], followed by rule-based automatic filtering and manual correction and validation to ensure an-

notation accuracy and consistency.

For content recognition, we cropped a total of 2.5 million sub-images of document elements based on the structure detection results, which were then annotated using Qwen2.5-VL-72B [1] and Gemini 2.5 Pro [13]. To further expand our datasets for table and formula recognition, we employed a rule-based method to filter out erroneous samples from the open-source datasets PubTabNet [60] and UniMER-1M [48]. Addressing the scarcity of Chinese data, we populated existing table structures with Chinese characters and rendered them into new table images. For formulas, we designed prompts to guide an LLM in generating commonly used Chinese formulas across various domains and also used the LLM to translate existing English formulas into Chinese, which were subsequently rendered. To enhance the diversity and authenticity of our table and formula data, we scraped LaTeX source from ArXiv, used an LLM to filter out irrelevant content, converted the tables to HTML format, and then rendered them into images.

For relation prediction, our goal is to construct a block-level reading order dataset that bridges the gap between existing block-level structure detection and line-level reading order prediction methods. First, we refined the existing open-source dataset [53] by linking tables and images to their corresponding captions and removing low-quality samples to improve annotation accuracy. Second, to address the scarcity of Chinese documents, we manually annotated a variety of Chinese document types, enriching the dataset’s diversity. Finally, to fully utilize the large amount of structure detection data with layout annotations but without reading order information, we adopted an automatic labeling strategy. This strategy first employs an OCR tool [21] to detect text lines within each block, then uses a line-level reading order model [50] to predict their sequence. The block-level reading order is then inferred by calculating the average reading order of all text lines within the block.

### 4. MonkeyOCR

Fig. 3 illustrates the overall pipeline of MonkeyOCR. First, the input image is fed into the structure detection model to

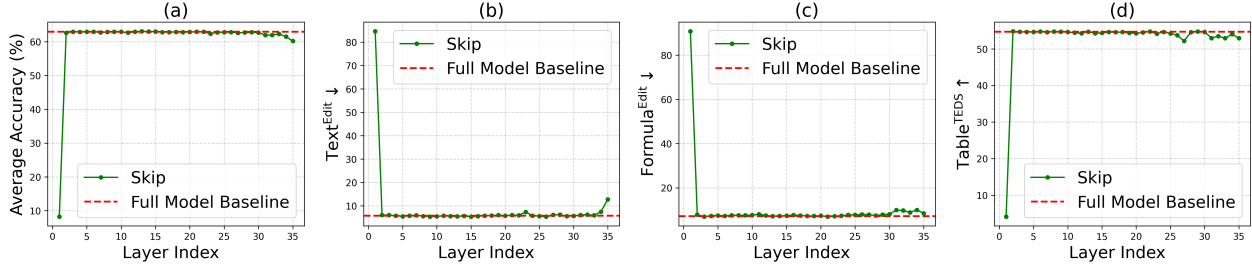


Figure 5. Results of MonkeyOCR-3B on text, formula, and table tasks. Green denotes skipping layer N, and red denotes no skipping.

obtain bounding boxes and categories for each document element. Based on these bounding boxes, the corresponding text, table, and formula regions are cropped and sent to an LMM for content recognition. Meanwhile, the coordinates and categories of the detected elements are passed to the relation prediction model to determine the reading order of the document elements. Finally, the recognized results are integrated according to the predicted reading order to produce the final structured document. The proposed SRR paradigm simplifies traditional pipeline-based methods into three unified models, thereby mitigating the cumulative errors caused by multiple tool combinations. Moreover, by processing document blocks in parallel, our method avoids the long context lengths associated with full-document processing, leading to substantial gains in speed. We also found parameter redundancy in large multimodal models and proposed the contiguous parameter degradation method, which enables faster inference with minimal performance degradation.

#### 4.1. Structure Detection

We employ DETR-based [56] model for structure detection, which consists of a backbone, an encoder, a query selection module, as well as a decoder and prediction heads. Given a document image  $I \in \mathbb{R}^{H \times W \times 3}$ , the backbone and encoder extracts visual features:

$$F_0 = \text{Backbone}(I), F_{\text{enc}} = \text{Encoder}(F_0), \quad (1)$$

where  $F_{\text{enc}} \in \mathbb{R}^{N \times C}$  represents the encoded feature tokens.

To estimate the likelihood of each token corresponding to a foreground region, a lightweight classification head is applied to  $F_{\text{enc}}$ :

$$s = \text{SiLU}(\text{BN}(\text{Conv}_{1 \times 1}(F_{\text{enc}}))), \quad (2)$$

where  $s$  represents the foreground probability of each token, indicating its likelihood of belonging to meaningful elements (e.g., text, table, figure).

Based on these scores, the query selection module picks the top- $K$  most informative features:

$$Q_0 = \text{TopK}(F_{\text{enc}}, s, K), \quad (3)$$

effectively filtering background noise and providing high-quality queries for the decoder.

Finally, the decoder refines the selected queries through iterative attention, followed by task-specific heads to produce the final layout predictions.

$$y = \text{Head}(\text{Decoder}(Q_0, F_0)), \quad (4)$$

where each prediction  $y_i = (b_i, l_i)$  includes a bounding box  $b_i$  and a category label  $l_i$ .

#### 4.2. Content Recognition

Given the detected bounding boxes  $B = \{b_1, b_2, \dots, b_n\}$ , each region is first cropped from the original document image  $I$  to obtain sub-images:

$$I_{\text{crop}}^i = \text{Crop}(I, b_i). \quad (5)$$

Each cropped image is preserved at its original resolution and then encoded into a sequence of visual tokens through a vision encoder followed by an MLP projection:

$$T_v^i = \text{MLP}(\text{VisionEnc}(I_{\text{crop}}^i)). \quad (6)$$

For each block, a type-specific prompt  $p_{l_i}$  is selected according to its predicted category  $l_i$  (e.g., text, table, or formula). Finally, the visual tokens and the corresponding prompt tokens are jointly fed into an LLM to produce the final content predictions:

$$C = \text{LLM}(\{T_v^1, \dots, T_v^n\}, \{p_{l_1}, \dots, p_{l_n}\}), \quad (7)$$

where  $C = \{c_1, c_2, \dots, c_n\}$  denotes the textual representations of the detected document elements.

#### 4.3. Relation Prediction

We build a block-level category-aware relation prediction model, which consists of embedding layers, transformer blocks and a classification layer. Given a bounding box  $b_i = (x_1, y_1, x_2, y_2)$  and its width and height, its positional embedding is computed as

$$P_i = \text{Concat}(E(p) \mid p \in \{x_1, y_1, x_2, y_2, w, h\}), \quad (8)$$

Model Type	Methods	Overall <sup>Edit</sup> ↓		Text <sup>Edit</sup> ↓		Formula <sup>Edit</sup> ↓		Table <sup>TEDS</sup> ↑		Table <sup>Edit</sup> ↓		Read Order <sup>Edit</sup> ↓	
		EN	ZH	EN	ZH	EN	ZH	EN	ZH	EN	ZH	EN	ZH
Pipeline Tools	MinerU [49]	0.150	0.357	0.061	0.215	0.278	0.577	78.6	62.1	0.180	0.344	0.079	0.292
	Marker [39]	0.336	0.556	0.080	0.315	0.530	0.883	67.6	49.2	0.619	0.685	0.114	0.340
	Mathpix [29]	0.191	0.365	0.105	0.384	0.306	0.454	77.0	67.1	0.243	0.320	0.108	0.304
	Docling [26]	0.589	0.909	0.416	0.987	0.999	1	61.3	25.0	0.627	0.810	0.313	0.837
	Pix2Text [4]	0.320	0.528	0.138	0.356	0.276	0.611	73.6	66.2	0.584	0.645	0.281	0.499
	Unstructured [45]	0.586	0.716	0.198	0.481	0.999	1	0	0.06	1	0.998	0.145	0.387
	OpenParse [12]	0.646	0.814	0.681	0.974	0.996	1	64.8	27.5	0.284	0.639	0.595	0.641
	PPStruct-V3 [9]	0.145	0.206	0.058	0.088	0.295	0.535	77.2	83.9	0.159	0.109	0.069	<b>0.091</b>
Expert VLMs	GOT-OCR [51]	0.287	0.411	0.189	0.315	0.360	0.528	53.2	47.2	0.459	0.520	0.141	0.280
	Nougat [3]	0.452	0.973	0.365	0.998	0.488	0.941	39.9	0	0.572	1.000	0.382	0.954
	Mistral OCR [31]	0.268	0.439	0.072	0.325	0.318	0.495	75.8	63.6	0.600	0.650	0.083	0.284
	OLMOCR [43]	0.326	0.469	0.097	0.293	0.455	0.655	68.1	61.3	0.608	0.652	0.145	0.277
	SmolDocling [34]	0.493	0.816	0.262	0.838	0.753	0.997	44.9	16.5	0.729	0.907	0.227	0.522
	Dolphin [11]	0.206	0.306	0.107	0.197	0.447	0.580	77.3	67.2	0.180	0.285	0.091	0.162
	MinerU2.0 [49]	0.139	0.240	0.047	0.109	0.297	0.536	82.5	79.0	0.141	0.195	0.069	0.118
	OCRFlux-3B [5]	0.195	0.281	0.064	0.183	0.379	0.613	71.6	81.3	0.253	0.139	0.086	0.187
	Nanonets-OCR-3B [28]	0.283	0.295	0.134	0.231	0.518	0.546	76.8	79.4	0.343	0.201	0.135	0.200
DeepSeekOCR-3B-Large [52]	0.138	0.208	0.054	0.143	0.277	0.461	-	-	0.152	0.104	0.067	0.123	
General VLMs	GPT4o [36]	0.233	0.399	0.144	0.409	0.425	0.606	72.0	62.9	0.234	0.329	0.128	0.251
	Qwen2.5-VL-7B [1]	0.312	0.406	0.157	0.228	0.351	0.574	76.4	72.2	0.588	0.619	0.149	0.203
	InternVL3-8B [6]	0.314	0.383	0.134	0.218	0.417	0.563	66.1	73.1	0.586	0.564	0.118	0.186
	Qwen2.5-VL-72B [1]	0.214	0.261	0.092	0.180	0.315	0.434	82.9	83.9	0.341	0.262	0.106	0.168
	Gemini2.5-Pro [13]	0.148	0.212	0.055	0.168	0.356	0.439	<b>85.8</b>	86.4	0.130	0.119	<b>0.049</b>	0.121
Mix	MonkeyOCR-1.2B	0.133	0.166	0.047	0.087	0.284	0.344	83.0	85.8	0.130	0.122	0.069	0.112
	MonkeyOCR-3B	<b>0.118</b>	<b>0.151</b>	<b>0.043</b>	<b>0.077</b>	<b>0.247</b>	<b>0.321</b>	84.2	<b>89.5</b>	<b>0.118</b>	<b>0.093</b>	0.066	0.113

Table 2. The end-to-end evaluation results of different tasks on OmniDocBench.

where  $E(\cdot)$  denotes separate embedding layers. Different types of document elements typically exhibit distinct semantic priorities for reading order. To explicitly capture this, we propose a category-aware embedding and combine it with positional encoding to construct more discriminative input features:

$$F_i = P_i + E_c(l_i), \quad (9)$$

where  $l_i$  denotes the category of the element.

The sequence of features  $[F_1, \dots, F_N]$  is processed by transformer layers to model contextual relationships, followed by a classification layer producing the reading order logits:

$$L = \text{Classifier}(\text{Transformer}([F_1, \dots, F_N])), \quad (10)$$

where  $L$  represents the predicted logits for each element’s position. The final reading order is obtained via iterative greedy decoding: each element is first assigned to its highest-scoring position; conflicts are resolved by retaining the element with the highest logit and reassigning others to their next-best positions. This process repeats until a valid permutation is obtained.

#### 4.4. Contiguous Parameter Degradation

In the field of document intelligence, document parsing serves as an upstream task where processing speed is critical. Since models with fewer parameters generally achieve faster inference, we pose the following question: *are all*

*layers in a large multimodal model truly necessary?* To investigate this, we randomly selected 50 samples from each of the three tasks: text recognition, formula recognition, and table recognition, for experimentation. We systematically pruned the LLM one layer at a time and evaluated the performance on each task. The results, shown in Fig. 5, reveal that removing the first layer of the LLM leads to a notable performance drop, whereas pruning other layers results in relatively minor degradation. This observation suggests that not all layers in the LLM are indispensable, and that certain parameters may be redundant. However, how to effectively prune the model remains a question. To this end, we conduct a systematic ablation study on different pruning strategies in Sec 5.3. Based on the results, we empirically propose contiguous parameter degradation, which directly prunes  $m$  contiguous middle layers of the LLM followed by fine-tuning. We hypothesize that adjacent layers in the LLM carry continuous and tightly coupled information. By performing contiguous pruning primarily on the middle layers, we can maximally preserve the continuity and semantic relationships between neighboring layers, thereby maintaining performance.

#### 4.5. Implement Details

MonkeyOCR is initialized from pretrained models [1, 8, 50] and subsequently undergoes large-scale training on MonkeyDoc. During the training process, we utilize the AdamW optimizer with a learning rate of  $2e-5$  and a cosine learning

Model Type	Models	Book	Slides	Financial Report	Textbook	Exam Paper	Magazine	Academic Papers	Notes	Newspaper	Overall
Pipeline Tools	MinerU [49]	<u>0.055</u>	0.124	0.033	0.102	0.159	<u>0.072</u>	<b>0.025</b>	0.984	0.171	0.206
	Marker [39]	0.074	0.340	0.089	0.319	0.452	0.153	0.059	0.651	0.192	0.274
	Mathpix [29]	0.131	0.220	0.202	0.216	0.278	0.147	0.091	0.634	0.690	0.300
Expert VLMs	GOT-OCR [51]	0.111	0.222	0.067	0.132	0.204	0.198	0.179	0.388	0.771	0.267
	Nougat [3]	0.734	0.958	1.000	0.820	0.930	0.830	0.214	0.991	0.871	0.806
	Dolphin [11]	0.091	0.131	0.057	0.146	0.231	0.121	0.074	0.363	0.307	0.177
	OCRFlux-3B [5]	0.068	0.125	0.092	0.102	0.119	0.083	0.047	0.223	0.536	0.149
General VLMs	GPT4o [36]	0.157	0.163	0.348	0.187	0.281	0.173	0.146	0.607	0.751	0.316
	Qwen2.5-VL-7B [1]	0.148	<b>0.053</b>	0.111	0.137	0.189	0.117	0.134	0.204	0.706	0.205
	InternVL3-8B [6]	0.163	<u>0.056</u>	0.107	0.109	0.129	0.100	0.159	<u>0.150</u>	0.681	0.188
Mix	<b>MonkeyOCR-1.2B</b>	<b>0.048</b>	0.079	<b>0.014</b>	<u>0.067</u>	<u>0.085</u>	<b>0.057</b>	0.042	0.184	<u>0.090</u>	<u>0.078</u>
	<b>MonkeyOCR-3B</b>	<b>0.048</b>	0.068	<u>0.015</u>	<b>0.063</b>	<b>0.080</b>	<b>0.057</b>	<u>0.040</u>	<b>0.120</b>	<b>0.083</b>	<b>0.067</b>

Table 3. The end-to-end text recognition performance on OmniDocBench across 9 PDF page types.

rate schedule. We employ a batch size of 64. Our 3B model was trained on 32 A800 GPUs.

## 5. Experiments

To validate the effectiveness of MonkeyOCR, we conducted a comprehensive comparison with both open-source and closed-source methods on OmniDocBench [37].

### 5.1. Comparison on Different Tasks

Document parsing encompasses a variety of sub-tasks, including text recognition, formula recognition, table recognition, reading order prediction, and more. To evaluate MonkeyOCR’s performance across these tasks, we compared it with widely-used methods on OmniDocBench [37], including pipeline tools [39, 49], expert VLMs [31, 51], closed-source general VLMs [36], and open-source general VLMs [1, 6]. As shown in Tab. 11, MonkeyOCR achieves the best overall performance on both Chinese and English document parsing tasks, attaining state-of-the-art results on 7 out of 10 sub-tasks. Specifically, our 3B model surpasses the best pipeline-based method PPStruct-V3, achieving a 13.1% improvement in formula recognition and outperforming the giant closed-source end-to-end model Gemini2.5-Pro. Moreover, our 1.2B model attains the second-best overall performance, outperforming both DeepSeekOCR-3B and Nanonets-OCR.

### 5.2. Comparison Across Document Types

As shown in Table 3, MonkeyOCR achieves the best overall performance. In particular, the MonkeyOCR-3B model outperforms both large-scale general VLMs and pipeline-based systems, exceeding InternVL3-8B [6] by 12.1% and MinerU [49] by 13.9% in overall performance. Remarkably, MonkeyOCR-1.2B model also delivers highly competitive results, ranking second overall with a score of 0.078, only 1.1% behind the 3B model. Beyond overall

performance, MonkeyOCR demonstrates strong robustness across different document categories, with the 3B model achieving the best results on seven types of documents. These results indicate that our model performs well across different document types.

### 5.3. Ablation Study

Method	Text <sup>Edit</sup> ↓	Formula <sup>Edit</sup> ↓	Table <sup>TEDS</sup> ↑	Order <sup>Edit</sup> ↓	Overall <sup>Edit</sup> ↓
Baseline	0.349	0.525	66.2	0.341	0.461
+SRR	0.071	0.333	81.0	0.157	0.175
+MonkeyDoc	<b>0.060</b>	<b>0.284</b>	<b>86.9</b>	<b>0.090</b>	<b>0.135</b>

Table 4. Ablation study on the proposed SRR paradigm and the MonkeyDoc dataset.

**Ablation study on SRR and MonkeyDoc.** We conducted experiments to systematically evaluate the effectiveness of the proposed SRR paradigm and the impact of training on the MonkeyDoc dataset. The baseline is the original Qwen2.5-VL-3B model with end-to-end prediction. As shown in Table 4, SRR significantly enhances the zero-shot document parsing performance of large multimodal models, achieving an average overall improvement of 28.6%, including a 27.8% gain in text recognition. This improvement can be attributed to SRR’s ability to mitigate interference from long contexts during inference. Moreover, after training on the MonkeyDoc dataset, the overall performance increases by 4%, with a 5.9% improvement in table recognition and a 6.7% improvement in reading order, demonstrating the effectiveness of the MonkeyDoc dataset.

**Impact of SRR paradigm on error accumulation.** To evaluate the effect of the proposed SRR paradigm on cumulative errors, we extended MonkeyOCR by incorporating text and formula detection models following the MinerU. Under this setup, text blocks are no longer fed directly into the LMM for recognition. Instead, word-level bounding boxes are first obtained via the detection models, and the

	Text <sup>Edit</sup> ↓		Formula <sup>Edit</sup> ↓		Overall <sup>Edit</sup> ↓	
	EN	ZH	EN	ZH	EN	ZH
SRR	0.043	0.077	0.247	0.321	0.118	0.151
+TD&FD	0.067	0.137	0.270	0.594	0.131	0.235

Table 5. Impact of SRR on error accumulation. “TD” and “FD” denote the text and formula detection models.

content within each box is then recognized by the LMM, with the results subsequently merged. As shown in Table 5, introducing these additional detection models leads to a decrease in text recognition by 4.2% and formula recognition by 14.8%, demonstrating the effectiveness of SRR in mitigating cumulative errors.

Model	3090	4090	A6000	H800	Avg.
MonkeyOCR-3B	0.497	1.006	0.609	0.897	0.752
MonkeyOCR-1.2B	0.677	1.436	0.825	1.101	1.010
Baseline-3B	0.244	0.387	0.285	0.518	0.359

Table 6. Inference speed (pages/s) comparison on different GPUs.

**Analysis of inference speed.** We randomly sampled 300 pages of PDFs from arXiv to analyze the inference speed of the models, with the results summarized in Tab. 6. Baseline-3B corresponds to Qwen2.5-VL-3B model fine-tuned on MonkeyDoc, which performs end-to-end prediction directly. The results show that MonkeyOCR-1.2B achieves a 34% speedup over MonkeyOCR-3B, while incurring only a 1.5% drop in performance. Furthermore, by enabling parallel block-wise prediction, MonkeyOCR-3B runs 2.09× faster than the fully end-to-end baseline, highlighting the efficiency advantage of the SRR paradigm.

	Text <sup>Edit</sup> ↓		Order <sup>Edit</sup> ↓		Overall <sup>Edit</sup> ↓	
	EN	ZH	EN	ZH	EN	ZH
Baseline	0.055	0.079	0.156	0.145	0.142	0.163
+BLRO	0.045	0.078	0.066	0.123	0.119	0.158
+CAE	0.043	0.077	0.066	0.113	0.118	0.151

Table 7. Ablation study on block-level reading order data (BLRO) and category-aware embedding (CAE).

**Ablation study on block-level reading order data and category-aware embedding.** The baseline model refers to LayoutReader [49], which only supports line-level reading order prediction. As shown in Tab. 7, training on our constructed block-level reading order data improves the model’s reading order performance for both Chinese and English by 5.6%. Incorporating category information into the original model further enhances reading order accuracy. Moreover, since the reading order prediction model does not affect the recognition results of other tasks, it only causes a minor impact on other tasks.

Strategy	Text <sup>Edit</sup> ↓	Formula <sup>Edit</sup> ↓	Table <sup>TEDS</sup> ↑	Overall <sup>Edit</sup> ↓
Train from scratch	0.120	0.355	65.2	0.208
Prune less important layers [30]	0.085	0.336	78.0	0.170
Prune deeper layers [14]	0.101	0.385	78.1	0.188
Prune shallow layers	0.091	0.363	77.9	0.180
CPD	<b>0.067</b>	<b>0.314</b>	<b>84.4</b>	<b>0.150</b>

Table 8. Ablation study on pruning strategies.

**Ablation study on pruning strategies.** Previous works [14, 30] have explored different strategies for pruning LLMs. Shortgpt [30] tends to prune less important layers, while prior work [14] favors pruning deeper layers (11-34). In addition, we further investigate the effects of pruning shallow layers (1-24) as well as training the LLM from scratch. As shown in Table 8, our proposed CPD outperforms training from scratch by 5.8% and surpasses the other pruning strategies.

Layers	Params	Text <sup>Edit</sup> ↓	Formula <sup>Edit</sup> ↓	Table <sup>TEDS</sup> ↑	Overall <sup>Edit</sup> ↓
36	3.0	0.060	0.284	86.9	0.135
12	1.2	0.067	0.314	84.4	0.150
8	0.9	0.076	0.321	78.3	0.164
4	0.6	0.091	0.340	74.9	0.180

Table 9. Ablation study on CPD.

**Ablation study on CPD.** We conduct an ablation study to investigate the impact of degree of parameter degradation on model performance. Specifically, we evaluate model variants retaining only 4, 8, and 12 layers of the original LLM. As shown in Tab. 9, retaining 12 layers results in only a marginal 1.5% overall performance drop. However, when only 4 layers are retained, performance on the text recognition decreases by 3.1%, while the more complex table recognition task suffers a significant 12% decline. These findings indicate that while smaller models are sufficient for simpler tasks, a larger parameter capacity is crucial for maintaining performance on complex tasks.

## 6. Conclusion

This paper introduces MonkeyOCR, a document parsing model based on the Structure-Recognition-Relation triplet paradigm, which unifies structural detection, content recognition, and relation prediction into a streamlined framework. This design simplifies traditional multi-tool pipelines while avoiding the inefficiencies of directly processing entire pages with LLMs, enabling both high accuracy and efficient deployment. We further identify parameter redundancy in large multimodal models and propose contiguous parameter degradation, which accelerates inference with minimal performance drop. Experiments show that MonkeyOCR achieves state-of-the-art performance on OmniDocBench, surpassing the closed-source commercial model Gemini2.5-Pro, demonstrating its potential as a foundation model for text-centric applications.

## References

- [1] Shuai Bai, Keqin Chen, Xuejing Liu, Jialin Wang, Wenbin Ge, Sibao Song, Kai Dang, Peng Wang, Shijie Wang, Jun Tang, Humen Zhong, Yuanzhi Zhu, Mingkun Yang, Zhao-hai Li, Jianqiang Wan, Pengfei Wang, Wei Ding, Zheren Fu, Yiheng Xu, Jiabo Ye, Xi Zhang, Tianbao Xie, Zesen Cheng, Hang Zhang, Zhibo Yang, Haiyang Xu, and Junyang Lin. Qwen2.5-vl technical report. *arXiv preprint arXiv:2502.13923*, 2025. 2, 3, 4, 6, 7, 13, 14, 16
- [2] Lukas Blecher. pix2tex - latex ocr. <https://github.com/lukas-blecher/LaTeX-OCR>, 2022. Accessed: 2024-02-29. 13
- [3] Lukas Blecher, Guillem Cucurull, Thomas Scialom, and Robert Stojnic. Nougat: Neural optical understanding for academic documents. *arXiv preprint arXiv:2308.13418*, 2023. 3, 6, 7
- [4] breezedeus. Pix2text: An open-source python3 tool for recognizing layouts, tables, math formulas (latex), and text in images. <https://github.com/breezedeus/pix2text>, 2025. 3, 6
- [5] ChatDoc. Ocrflux. <https://github.com/chatdoc-com/OCRFlux>, 2025. 3, 6, 7
- [6] Zhe Chen, Jiannan Wu, Wenhai Wang, Weijie Su, Guo Chen, Sen Xing, Muyan Zhong, Qinglong Zhang, Xizhou Zhu, Lewei Lu, et al. Internvl: Scaling up vision foundation models and aligning for generic visual-linguistic tasks. In *Proceedings of the IEEE/CVF conference on computer vision and pattern recognition*, pages 24185–24198, 2024. 3, 6, 7, 14, 16
- [7] Hiuyi Cheng, Peirong Zhang, Sihang Wu, Jiabin Zhang, Qiyuan Zhu, Zecheng Xie, Jing Li, Kai Ding, and Lianwen Jin. M6doc: a large-scale multi-format, multi-type, multi-layout, multi-language, multi-annotation category dataset for modern document layout analysis. In *Proceedings of the IEEE/CVF Conference on Computer Vision and Pattern Recognition*, pages 15138–15147, 2023. 3, 4, 12
- [8] Cheng Cui, Ting Sun, Suyin Liang, Tingquan Gao, Zelun Zhang, Jiakuan Liu, Xueqing Wang, Changda Zhou, Hongen Liu, Manhui Lin, Yue Zhang, Yubo Zhang, Handong Zheng, Jing Zhang, Jun Zhang, Yi Liu, Dianhai Yu, and Yanjun Ma. <https://huggingface.co/PaddlePaddle/PP-DocLayoutV2>, 2025. 6
- [9] Cheng Cui, Ting Sun, Manhui Lin, Tingquan Gao, Yubo Zhang, Jiakuan Liu, Xueqing Wang, Zelun Zhang, Changda Zhou, Hongen Liu, et al. Paddleocr 3.0 technical report. *arXiv preprint arXiv:2507.05595*, 2025. 2, 4, 6, 16
- [10] Cheng Da, Chuwei Luo, Qi Zheng, and Cong Yao. Vision grid transformer for document layout analysis. In *Proceedings of the IEEE/CVF international conference on computer vision*, pages 19462–19472, 2023. 3, 4, 12
- [11] Hao Feng, Shu Wei, Xiang Fei, Wei Shi, Yingdong Han, Lei Liao, Jinghui Lu, Binghong Wu, Qi Liu, Chunhui Lin, Jingqun Tang, Hao Liu, and Can Huang. Dolphin: Document image parsing via heterogeneous anchor prompting. In *Findings of the Association for Computational Linguistics, ACL 2025, Vienna, Austria, July 27 - August 1, 2025*, pages 21919–21936. Association for Computational Linguistics, 2025. 6, 7
- [12] Sergey Filimonov. Open parse: Visually-driven document chunking for llm applications. <https://github.com/Filimoa/open-parse>, 2025. 6
- [13] Google DeepMind. Gemini 2.5. <https://blog.google/technology/google-deepmind/gemini-model-thinking-updates-march-2025/>, 2025. 4, 6, 13
- [14] Andrey Gromov, Kushal Tirumala, Hassan Shapourian, Paolo Glorioso, and Daniel A. Roberts. The unreasonable ineffectiveness of the deeper layers. In *International conference on learning representations*, 2025. 8
- [15] Zhangxuan Gu, Changhua Meng, Ke Wang, Jun Lan, Weiqiang Wang, Ming Gu, and Liqing Zhang. Xylayoutlm: Towards layout-aware multimodal networks for visually-rich document understanding. In *Proceedings of the IEEE/CVF Conference on Computer Vision and Pattern Recognition (CVPR)*, pages 4583–4592, 2022. 3
- [16] Yelin He, Xianbiao Qi, Jiaquan Ye, Peng Gao, Yihao Chen, Bingcong Li, Xin Tang, and Rong Xiao. Pingan-vcgroup’s solution for icdar 2021 competition on scientific table image recognition to latex. *ArXiv*, abs/2105.01846, 2021. 3
- [17] Yupan Huang, Tengchao Lv, Lei Cui, Yutong Lu, and Furu Wei. Layoutlmv3: Pre-training for document ai with unified text and image masking. In *Proceedings of the 30th ACM international conference on multimedia*, pages 4083–4091, 2022. 3
- [18] Jaided AI. Easyocr: Ready-to-use ocr with 80+ supported languages. <https://github.com/JaidedAI/EasyOCR>, 2024. 3
- [19] Glenn Jocher, Ayush Chaurasia, and Jing Qiu. Ultralytics yolov8. <https://github.com/ultralytics/ultralytics>, 2023. 3
- [20] Geewook Kim, Teakgyu Hong, Moonbin Yim, Jeongyeon Nam, Jinyoung Park, Jinyeong Yim, Wonseok Hwang, Sangdoon Yun, Dongyoon Han, and Seunghyun Park. Ocr-free document understanding transformer. In *European Conference on Computer Vision*, pages 498–517. Springer, 2022. 3
- [21] Chenxia Li, Weiwei Liu, Ruoyu Guo, Xiaoting Yin, Kaitao Jiang, Yongkun Du, Yuning Du, Lingfeng Zhu, Baohua Lai, Xiaoguang Hu, et al. Pp-ocrv3: More attempts for the improvement of ultra lightweight ocr system. *arXiv preprint arXiv:2206.03001*, 2022. 3, 4, 14
- [22] Hang Li. Cdla: A chinese document layout analysis (cdla) dataset. <https://github.com/buptlihang/CDLA>, 2021. 3, 4, 12
- [23] Zhang Li, Biao Yang, Qiang Liu, Zhiyin Ma, Shuo Zhang, Jingxu Yang, Yabo Sun, Yuliang Liu, and Xiang Bai. Monkey: Image resolution and text label are important things for large multi-modal models. In *proceedings of the IEEE/CVF conference on computer vision and pattern recognition*, pages 26763–26773, 2024. 3
- [24] Yuliang Liu, Jiabin Zhang, Dezhi Peng, Mingxin Huang, Xinyu Wang, Jingqun Tang, Can Huang, Dahua Lin, Chunhua Shen, Xiang Bai, et al. Spts v2: single-point scene text

- spotting. *IEEE Transactions on Pattern Analysis and Machine Intelligence*, 45(12):15665–15679, 2023. 3
- [25] Yuliang Liu, Biao Yang, Qiang Liu, Zhang Li, Zhiyin Ma, Shuo Zhang, and Xiang Bai. Textmonkey: An ocr-free large multimodal model for understanding document. *arXiv preprint arXiv:2403.04473*, 2024. 3
- [26] Nikolaos Livathinos, Christoph Auer, Maksym Lysak, Ahmed Nassar, Michele Dolfi, Panos Vagenas, Cesar Berrospi Ramis, Matteo Omenetti, Kasper Dinkla, Yusik Kim, et al. Docling: An efficient open-source toolkit for ai-driven document conversion. *arXiv preprint arXiv:2501.17887*, 2025. 3, 6
- [27] Mahshad Mahdavi, Richard Zanibbi, Harold Mouchere, Christian Viard-Gaudin, and Utpal Garain. Icdar 2019 crohme+ tfd: Competition on recognition of handwritten mathematical expressions and typeset formula detection. In *2019 International Conference on Document Analysis and Recognition (ICDAR)*, pages 1533–1538. IEEE, 2019. 13
- [28] Souvik Mandal, Ashish Talewar, Paras Ahuja, and Prathamesh Juvatkar. Nanonets-ocr-s: A model for transforming documents into structured markdown with intelligent content recognition and semantic tagging. <https://huggingface.co/nanonets/Nanonets-OCR-s>, 2025. 3, 6
- [29] Mathpix. Mathpix snip: Convert images and pdfs to latex, docx, and more. <https://mathpix.com/>, 2025. 6, 7
- [30] Xin Men, Mingyu Xu, Qingyu Zhang, Qianhao Yuan, Bingning Wang, Hongyu Lin, Yaojie Lu, Xianpei Han, and Weipeng Chen. Shortgpt: Layers in large language models are more redundant than you expect. In *Findings of the Association for Computational Linguistics: ACL 2025*, pages 20192–20204, 2025. 8
- [31] Mistral OCR. Mistral ocr: Free online ai ocr tool to extract text. <https://www.mistralocr.com/>, 2025. 6, 7
- [32] Harold Mouchere, Christian Viard-Gaudin, Richard Zanibbi, and Utpal Garain. Icfhr 2014 competition on recognition of on-line handwritten mathematical expressions (crohme 2014). In *2014 14th International Conference on Frontiers in Handwriting Recognition*, pages 791–796. IEEE, 2014. 13
- [33] Harold Mouchère, Christian Viard-Gaudin, Richard Zanibbi, and Utpal Garain. Icfhr2016 crohme: Competition on recognition of online handwritten mathematical expressions. In *2016 15th International Conference on Frontiers in Handwriting Recognition (ICFHR)*, pages 607–612. IEEE, 2016. 13
- [34] Ahmed Nassar, Andres Marafioti, Matteo Omenetti, Maksym Lysak, Nikolaos Livathinos, Christoph Auer, Lucas Morin, Rafael Teixeira de Lima, Yusik Kim, A Said Gurbuz, et al. Smoldocling: An ultra-compact vision-language model for end-to-end multi-modal document conversion. *arXiv preprint arXiv:2503.11576*, 2025. 6
- [35] OleehyO. Texteller: An end-to-end formula recognition model. <https://github.com/OleehyO/TextTeller>, 2025. 4
- [36] OpenAI. Hello gpt-4o. <https://openai.com/index/hello-gpt-4o>, 2024. 6, 7
- [37] Linke Ouyang, Yuan Qu, Hongbin Zhou, Jiawei Zhu, Rui Zhang, Qunshu Lin, Bin Wang, Zhiyuan Zhao, Man Jiang, Xiaomeng Zhao, et al. Omnidocbench: Benchmarking diverse pdf document parsing with comprehensive annotations. In *Proceedings of the Computer Vision and Pattern Recognition Conference*, pages 24838–24848, 2025. 1, 7
- [38] Inkit Padhi, Yair Schiff, Igor Melnyk, Mattia Rigotti, Youssef Mroueh, Pierre Dognin, Jerret Ross, Ravi Nair, and Erik Altman. Tabular transformers for modeling multivariate time series. In *ICASSP 2021-2021 IEEE International Conference on Acoustics, Speech and Signal Processing (ICASSP)*, pages 3565–3569. IEEE, 2021. 3
- [39] Vik Paruchuri. Marker. <https://github.com/datalab-to/marker>, 2024. 3, 6, 7
- [40] Vikas Paruchuri and Datalab Team. Surya: A lightweight document ocr and analysis toolkit. <https://github.com/VikParuchuri/surya>, 2025. GitHub repository. 3
- [41] Dezhi Peng, Xinyu Wang, Yuliang Liu, Jiabin Zhang, Mingxin Huang, Songxuan Lai, Jing Li, Shenggao Zhu, Dahua Lin, Chunhua Shen, et al. Spts: single-point text spotting. In *Proceedings of the 30th ACM International Conference on Multimedia*, pages 4272–4281, 2022. 3
- [42] Birgit Pfitzmann, Christoph Auer, Michele Dolfi, Ahmed S Nassar, and Peter Staar. Doclaynet: A large human-annotated dataset for document-layout segmentation. In *Proceedings of the 28th ACM SIGKDD conference on knowledge discovery and data mining*, pages 3743–3751, 2022. 3, 4, 12
- [43] Jake Poznanski, Jon Borchardt, Jason Dunkelberger, Regan Huff, Daniel Lin, Aman Rangapur, Christopher Wilhelm, Kyle Lo, and Luca Soldaini. olmocr: Unlocking trillions of tokens in pdfs with vision language models. *arXiv preprint arXiv:2502.18443*, 2025. 3, 6
- [44] Qwen, :, An Yang, Baosong Yang, Beichen Zhang, Binyuan Hui, Bo Zheng, Bowen Yu, Chengyuan Li, Dayiheng Liu, Fei Huang, Haoran Wei, Huan Lin, Jian Yang, Jianhong Tu, Jianwei Zhang, Jianxin Yang, Jiayi Yang, Jingren Zhou, Junyang Lin, Kai Dang, Keming Lu, Keqin Bao, Kexin Yang, Le Yu, Mei Li, Mingfeng Xue, Pei Zhang, Qin Zhu, Rui Men, Runji Lin, Tianhao Li, Tianyi Tang, Tingyu Xia, Xingzhang Ren, Xuancheng Ren, Yang Fan, Yang Su, Yichang Zhang, Yu Wan, Yuqiong Liu, Zeyu Cui, Zhenru Zhang, and Zihan Qiu. Qwen2.5 technical report, 2025. 13, 14
- [45] Unstructured-IO. Unstructured: Open-source etl for complex document transformation. <https://github.com/Unstructured-IO/unstructured>, 2025. 6
- [46] Jianqiang Wan, Sibong Song, Wenwen Yu, Yuliang Liu, Wenqing Cheng, Fei Huang, Xiang Bai, Cong Yao, and Zhibo Yang. Omniparser: A unified framework for text spotting key information extraction and table recognition. In *Proceedings of the IEEE/CVF Conference on Computer Vision and Pattern Recognition*, pages 15641–15653, 2024. 3
- [47] Ao Wang, Hui Chen, Lihao Liu, Kai Chen, Zijia Lin, Jungong Han, et al. Yolov10: Real-time end-to-end object detection. *Advances in Neural Information Processing Systems*, 37:107984–108011, 2024. 3
- [48] Bin Wang, Zhuangcheng Gu, Guang Liang, Chao Xu, Bo Zhang, Botian Shi, and Conghui He. Unimernet: A universal

- network for real-world mathematical expression recognition. *arXiv preprint arXiv:2404.15254*, 2024. 3, 4, 13
- [49] Bin Wang, Chao Xu, Xiaomeng Zhao, Linke Ouyang, Fan Wu, Zhiyuan Zhao, Rui Xu, Kaiwen Liu, Yuan Qu, Fukai Shang, et al. Mineru: An open-source solution for precise document content extraction. *arXiv preprint arXiv:2409.18839*, 2024. 2, 3, 6, 7, 8, 16
- [50] Zilong Wang, Yiheng Xu, Lei Cui, Jingbo Shang, and Furu Wei. Layoutreader: Pre-training of text and layout for reading order detection. In *Proceedings of the 2021 Conference on Empirical Methods in Natural Language Processing*, pages 4735–4744, 2021. 3, 4, 6, 14
- [51] Haoran Wei, Chenglong Liu, Jinyue Chen, Jia Wang, Lingyu Kong, Yanming Xu, Zheng Ge, Liang Zhao, Jianjian Sun, Yuang Peng, et al. General ocr theory: Towards ocr-2.0 via a unified end-to-end model. 2024. 3, 6, 7
- [52] Haoran Wei, Yaofeng Sun, and Yukun Li. Deepseek-ocr: Contexts optical compression. *arXiv preprint arXiv:2510.18234*, 2025. 3, 6
- [53] Renqiu Xia, Song Mao, Xiangchao Yan, Hongbin Zhou, Bo Zhang, Haoyang Peng, Jiahao Pi, Daocheng Fu, Wenjie Wu, Hancheng Ye, et al. Docgenome: An open large-scale scientific document benchmark for training and testing multi-modal large language models. *arXiv preprint arXiv:2406.11633*, 2024. 3, 4, 13
- [54] Jiaquan Ye, Xianbiao Qi, Yelin He, Yihao Chen, Dengyi Gu, Peng Gao, and Rong Xiao. Pingan-vcgroup’s solution for icdar 2021 competition on scientific literature parsing task b: Table recognition to html. *arXiv preprint arXiv:2105.01848*, 2021. 3
- [55] Ye Yuan, Xiao Liu, Wondimu Dikubab, Hui Liu, Zhilong Ji, Zhongqin Wu, and Xiang Bai. Syntax-aware network for handwritten mathematical expression recognition. In *Proceedings of the IEEE/CVF conference on computer vision and pattern recognition*, pages 4553–4562, 2022. 3, 13
- [56] Yian Zhao, Wenyu Lv, Shangliang Xu, Jinman Wei, Guanzhong Wang, Qingqing Dang, Yi Liu, and Jie Chen. Detsr beat yolos on real-time object detection. In *Proceedings of the IEEE/CVF conference on computer vision and pattern recognition*, pages 16965–16974, 2024. 3, 5
- [57] Zhiyuan Zhao, Hengrui Kang, Bin Wang, and Conghui He. Doclayout-yolo: Enhancing document layout analysis through diverse synthetic data and global-to-local adaptive perception. *arXiv preprint arXiv:2410.12628*, 2024. 3, 4
- [58] Ge Zheng, Jiaye Qian, Jiajin Tang, and Sibe Yang. Why llms are more prone to hallucinations in longer responses: The role of context. In *Proceedings of the IEEE/CVF International Conference on Computer Vision*, pages 4101–4113, 2025. 2
- [59] Xinyi Zheng, Douglas Burdick, Lucian Popa, Xu Zhong, and Nancy Xin Ru Wang. Global table extractor (gte): A framework for joint table identification and cell structure recognition using visual context. In *Proceedings of the IEEE/CVF winter conference on applications of computer vision*, pages 697–706, 2021. 3, 4
- [60] Xu Zhong, Elaheh ShafieiBavani, and Antonio Jimeno Yepes. Image-based table recognition: data, model, and evaluation. In *European conference on computer vision*, pages 564–580. Springer, 2020. 3, 4, 13
- [61] Yiyang Zhou, Chenhang Cui, Jaehong Yoon, Linjun Zhang, Zhun Deng, Chelsea Finn, Mohit Bansal, and Huaxiu Yao. Analyzing and mitigating object hallucination in large vision-language models. In *International Conference on Learning Representations*, 2024. 2

## A. MonkeyDoc Dataset

MonkeyDoc is designed to cover a complete range of document parsing tasks, including layout detection, reading order prediction, text recognition, table recognition, formula recognition, and code block recognition. As shown in Fig. 6, MonkeyDoc spans more than ten diverse document domains and provides high-quality annotations in both Chinese and English, making it a comprehensive and versatile dataset for document parsing. In comparison, previous datasets are often limited to a subset of tasks, a single document type, or monolingual settings. MonkeyDoc uniquely enables multi-task, multi-domain, and bilingual training and evaluation, supporting both fine-grained and holistic document understanding. In the following sections, we provide a detailed description of the data construction process for each stage.

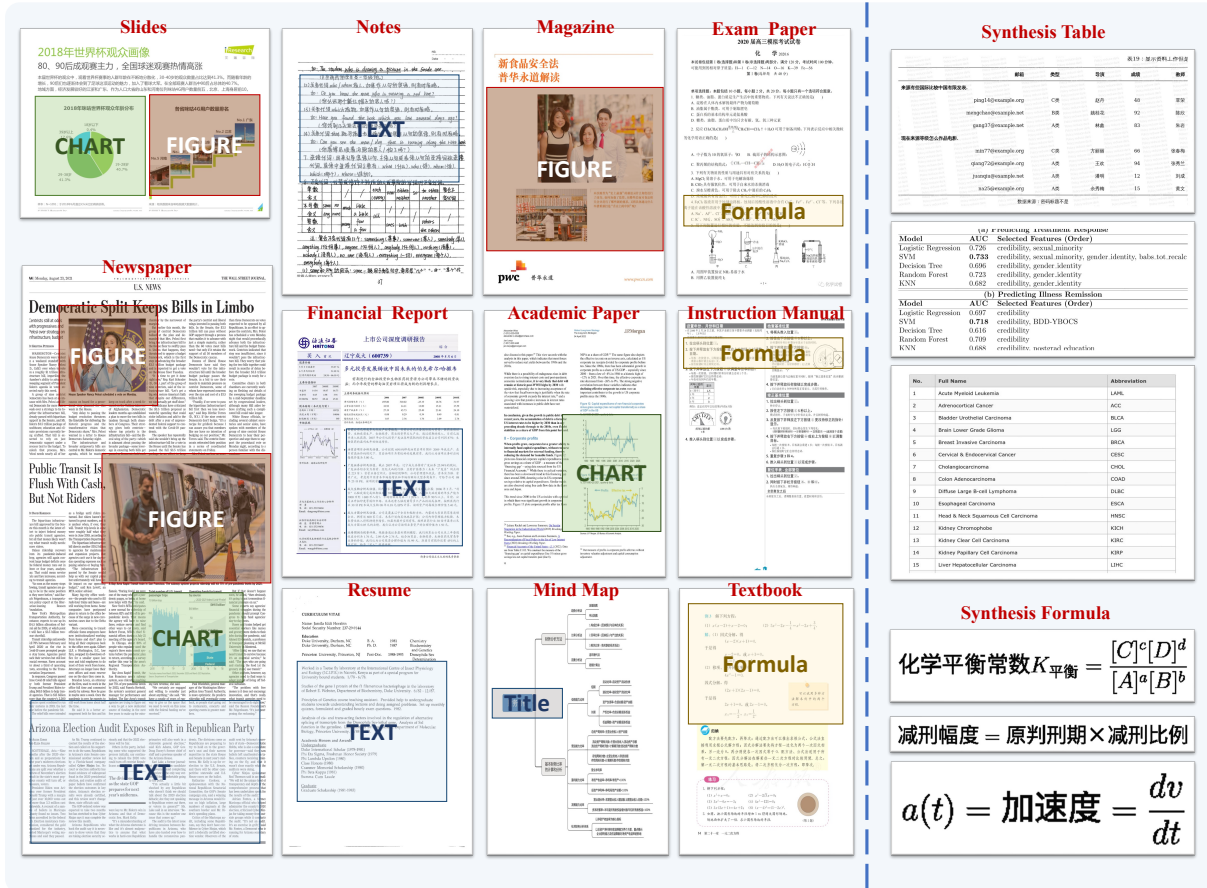


Figure 6. Visualization of the MonkeyDoc dataset. MonkeyDoc encompasses more than ten document types and includes our synthesized tables and formulas data.

### A.1. Structure Detection

The task of Structure Detection involves detecting elements such as text, tables, and images within a document and returning their corresponding categories and bounding box coordinates. To construct the Structure Detection dataset, we focus on two main aspects:

**Filtering from Open-Source Datasets.** We collect existing open-source Structure Detection datasets, including M<sup>6</sup>Doc [7], DocLayNet [42], D4LA [10], and CDLA [22], covering both Chinese and English documents, with a total of 153k pages. We process and filter the original annotations by removing nested bounding boxes and retaining only the largest bounding box along with its category and coordinates. Additionally, we compute the proportion of each bounding box’s area relative to the total page area and remove low-information instances where this ratio is less than 35%. To address the inconsistency in category annotations across different datasets (e.g., M<sup>6</sup>Doc [7] defines 74 categories while D4LA [10] uses 27), we map all category labels to a unified set of classes.

**Synthesizing Chinese Data.** Given the scarcity of Chinese samples in existing open-source datasets, we further collected over 300k pages of Chinese documents spanning financial reports, textbooks, academic papers, and more. These pages were first pre-annotated using an existing Structure Detection model, followed by rule-based post-processing—such as removing nested bounding boxes and filtering low-information instances—and subsequent manual correction and verification to ensure annotation accuracy and consistency. In total, these steps yield 150k high-quality samples.

## A.2. Content Recognition

Content recognition includes text block recognition, table recognition, formula recognition, and code block recognition. To construct data for these tasks, we focus on four key components:

**Cropping Document Elements.** Leveraging the layouts obtained from Structure Detection, we extracted various types of document elements from the images, yielding a total of 2.5 million cropped samples. Text blocks, formula blocks, and tables were annotated using the advanced model Qwen2.5VL-72B [1] as well as the commercial tool Gemini2.5Pro [13].

**Filtering from Open-Source Datasets.** For table recognition, we filter data from PubTabNet [60] through a series of quality checks, including verifying HTML tag closure, ensuring table structure completeness (e.g., presence of headers), validating the correctness of merged cells, checking header-body alignment, detecting abnormal encoded characters, and performing overall syntax validation. This results in a clean dataset of 470k tables. For formula recognition, we use the UniMER-1M [48] dataset as the training set, which is constructed from diverse sources, including public datasets such as Pix2tex [2], CROHME [27, 32, 33] and HME100K [55], as well as LaTeX expressions collected from Arxiv, Wikipedia and StackExchange. The dataset includes printed, handwritten and screen-captured formulas, ensuring broad coverage of expression styles and complexities. In total, it contains approximately 1.5 million samples.

**Synthesizing Chinese Data.** Due to the limited availability of Chinese data for table and formula recognition, we manually synthesize additional datasets. For tables, we collect numerous existing table structures featuring diverse multi-row, multi-column, and nested combinations, automatically populate table cells with Chinese characters, and render the results into Chinese table images paired with HTML annotations. For formulas, we synthesize the dataset through two approaches: first, by using large multimodal models to generate commonly used formulas in Chinese across various industries; second, by translating English formulas from the UniMER-1M [48] dataset into Chinese using large language models and rendering them into Chinese formula images. In total, the synthesized Chinese tables and formulas comprise 135k samples.

**ArXiv Data Extraction.** To further enrich the dataset, we crawl LaTeX data for tables and formulas from ArXiv. The crawled data is processed using the advanced open-source large language model Qwen2.5-72B [44] to filter out unnecessary elements such as citations and comments. Additionally, table LaTeX data is converted into HTML using these models and then rendered into images. This ensures the inclusion of high-quality academic data into the dataset, resulting in a total of 411k collected samples.

By combining these four steps, we build a comprehensive and diverse dataset for content recognition, supporting text block, table and formula identification in both Chinese and English.

## A.3. Relation Prediction

Based on the completed structure detection and content recognition, we further predict the reading order relationships between elements. Existing structure detection models output region-level bounding boxes, which are not directly compatible with line-level reading order prediction models. To bridge this gap, we construct a region-level reading order dataset to train models specifically for this granularity. We collect three types of data for reading order construction: open-source datasets with region level reading order annotations, unlabeled Chinese data with diverse document types, and documents with region level layout annotations, and design dedicated strategies for each.

**Filtering from Open-Source Datasets.** To our knowledge, DocGenome [53] is the only open-source training dataset that provides region-level reading order annotations. These annotations are generated through an automated labeling process, which may introduce a certain degree of inaccuracy. To address potential inaccuracies or omissions in the reading order annotations for images and tables, we refine the annotations by strictly associating each image and table with its corresponding caption. We then filter out low-quality data, including pages with unannotated regions or excessive blank areas. After completing the correction and filtering steps, we score samples based on the diversity of element types on each page, incorporating high-scoring pages into our training set. As a result, we obtain 951k samples with high-quality reading order annotations.

**Manually Annotating Chinese Data.** Given the scarcity of Chinese documents in existing datasets, we collected a wide range of Chinese document types, including research reports, academic papers, user manuals, books, test papers, slides, official documents, newspapers and journals, as well as contracts. We manually annotated the region-level reading order of

these documents, resulting in 154k samples, to enhance the coverage and diversity of Chinese scenarios in the dataset.

**Automatic Annotation with Expert Models.** Existing layout analysis datasets typically provide region-level bounding box annotations but lack corresponding reading order information. To address this limitation, we leverage the bounding box annotations from these datasets and the line-level LayoutReader [50] model to automatically generate region-level reading order labels. Specifically, we first utilize PPOCR [21] to perform line-wise text recognition within each bounding box, obtaining the positional information of all text lines. Subsequently, LayoutReader predicts the reading order of these text lines. Finally, the region-level reading order is determined by calculating the average predicted order of all text lines within the region. This process produces 228k region-level reading order annotations, effectively enhancing existing layout datasets.

Tab. C	Text	Table	Formula
1-NED	99.6	99.96	99.1

Table 10. Comparison between automatically generated annotations and manually corrected ground truth.

#### A.4. Comparison with Human Annotation.

We implemented a strict quality control procedure for annotation generation. Prior to large-scale generation, we annotated a small subset of samples and manually verified whether the accuracy met our predefined standards. During this pilot phase, we observed that Qwen2.5VL-72B did not achieve satisfactory performance on table recognition. Therefore, we used Qwen2.5VL-72B exclusively for annotating text and formulas, while tables were annotated using Gemini 2.5-Pro and supplemented with automatically synthesized and rendered table data. After the full dataset was generated, we randomly sampled a substantial portion of instances for manual inspection to identify potential errors. For systematic and recurring errors, we applied rule-based filtering strategies to further refine the annotations. Finally, we randomly selected 100 instances each of text, tables, and formulas for validation. We computed the 1-NED between the original annotations and the manually corrected ground truth, as reported in Tab. 10.

Vision Encoder	LLM	Overall <sup>Edit</sup> ↓		Text <sup>Edit</sup> ↓		Formula <sup>Edit</sup> ↓		Table <sup>TEDS</sup> ↑		Table <sup>Edit</sup> ↓		Read Order <sup>Edit</sup> ↓	
		EN	ZH	EN	ZH	EN	ZH	EN	ZH	EN	ZH	EN	ZH
QwenVit	Qwen2.5-3B	0.118	0.151	0.043	0.077	0.247	0.321	84.2	89.5	0.118	0.093	0.066	0.113
QwenVit	Qwen3-1.7B	0.131	0.149	0.044	0.074	0.293	0.326	84.7	87.9	0.125	0.087	0.062	0.110
InternVit	Qwen3-0.6B	0.144	0.176	0.116	0.154	0.263	0.328	83.8	87.9	0.128	0.112	0.070	0.110

Table 11. The end-to-end evaluation results of different backbones on OmniDocBench.

## B. MonkeyOCR with Different Backbones

We further analyze the performance of MonkeyOCR under different backbone configurations. Specifically, we evaluate multiple encoders (such as QwenViT [1] and InternViT [6]) and LLMs of varying scales (Qwen2.5-3B [44], Qwen3-1.7B, and Qwen3-0.6B) trained on MonkeyDoc. Experimental results show that the proposed SRR paradigm and the MonkeyDoc dataset exhibit strong robustness across all backbone settings. Moreover, backbone configurations with larger parameter sizes generally achieve better overall performance.

## C. Comparison on OmniDocBench v1.5

We further conduct comparisons with other models on OmniDocBench v1.5, which contains 1,355 document images with a more balanced distribution of document and element types. In this updated benchmark, formula recognition is evaluated using the CDM metric. As shown in Tab. 12, our model demonstrates strong performance.

## D. Non-Manhattan Layouts

We visualize our model’s results on non-rectangular text blocks (Fig. 7 (a)), artistic magazine (Fig. 7 (b)), and paragraph overlapping QR code (Fig. 7 (c)). Non-rectangular text blocks are detected as rectangular regions; in Fig. 7 (b), image order does not affect textual semantics, allowing correct reading order. We do not flag improperly cropped characters, and when

Model	Overall $\uparrow$	Text <sup>Edit</sup> $\downarrow$	Formula <sup>CDM</sup> $\uparrow$	Table <sup>TEDS</sup> $\uparrow$	Table <sup>TEDS-S</sup> $\uparrow$	Read Order <sup>Edit</sup> $\downarrow$
MonkeyOCR-3B	91.02	0.049	89.51	88.43	92.74	0.074
MinerU2.5	90.67	0.047	88.46	88.22	92.38	0.044
dots.ocr	88.41	0.048	83.22	86.78	90.62	0.053
Deepseek-OCR	87.01	0.073	83.37	84.97	88.80	0.086

Table 12. Comprehensive evaluation of document parsing on OmniDocBench v1.5.

structure detection fails, we perform end-to-end recognition on the full page. To avoid overlap in Fig. 7 (c) (5,6,7), the paragraph is split into two blocks.

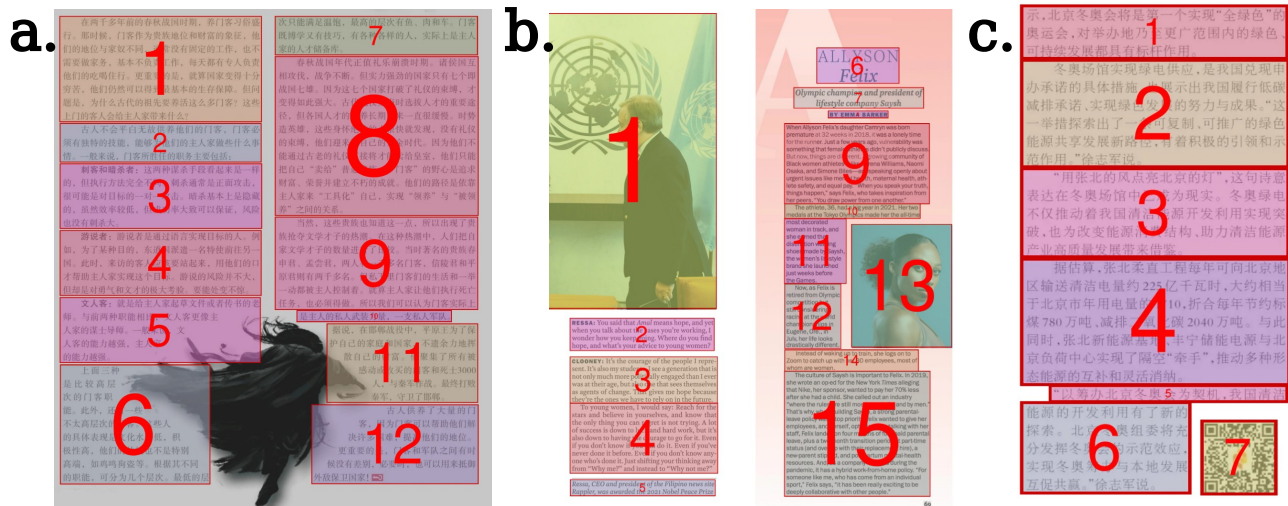


Figure 7. Visualization results on non-Manhattan layouts.

## E. More analysis of CPD

To further analyze the advantages of CPD, we sampled a subset of the training data to compare CPD with traditional knowledge distillation (KD). Specifically, we initialized the LLM with selected layers from Qwen2.5-3B and used MonkeyOCR-3B as the teacher to train the 1.2B model. Since KD requires additional inference from the 3B model, CPD achieves approximately three times higher training efficiency. Under the same training setup, CPD outperforms KD by 2.17%. We also examined how the smaller 1.2B model performs across different tasks. For simple tasks, its performance drops only slightly compared to the 3B model, whereas more complex tasks such as formula recognition and table recognition suffer a larger decline. This difference is likely because text recognition only requires content transcription, while tables and formulas involve intricate structures that demand deeper understanding. Visualizing typical failure cases after pruning, we found that errors mainly occur in table and formula structures—for instance, the model misreads table cells (Fig. 8 (a)) and interprets fractions incorrectly as left-right sequences (Fig. 8 (b)).

## F. Limitations

Pipeline methods (e.g., PPOCR, MinerU) first perform layout detection, followed by text and formula detection, instance-level recognition, merging of recognized elements, and reading-order reconstruction. These approaches rely on at least seven specialized models and complex post-processing. In contrast, our method unifies the process under a triplet paradigm, achieving a significantly better accuracy-efficiency trade-off. Although cumulative errors cannot be fully eliminated, our method substantially mitigates them while remaining efficient. Unlike pipeline methods that detect individual text instances, our model detects element blocks. Statistics show that inter-block spacing is larger than inter-text spacing (5.2 mm vs. 1.5 mm), making block-level detection more robust. On OmniDocBench v1.5, MinerU produces an average of 97.2 boxes per

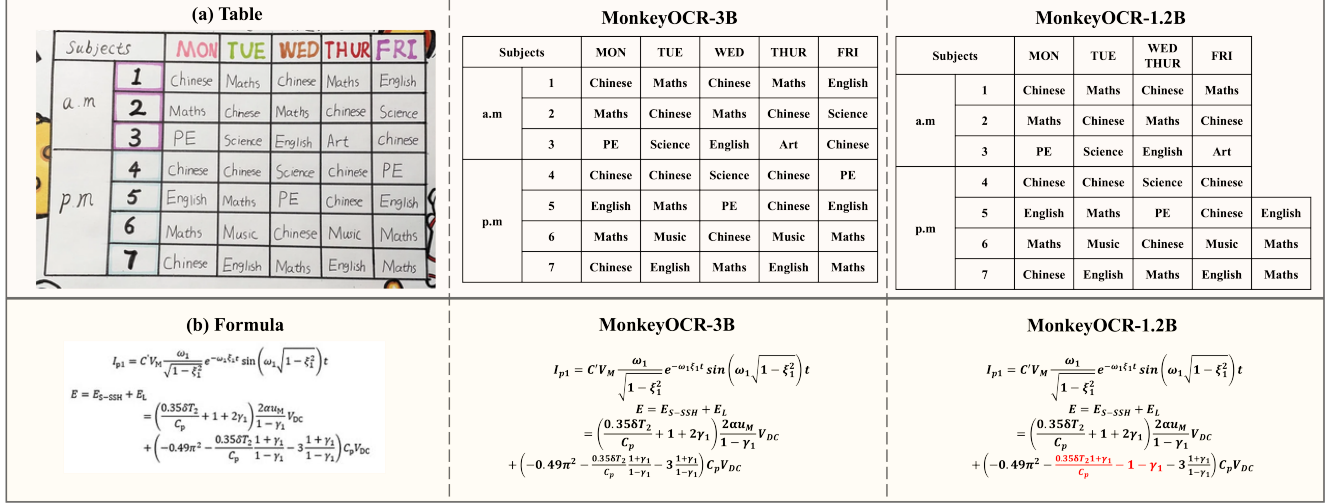


Figure 8. Typical failure cases.

image, compared to 19.5 for our method. Furthermore, since reading order in some documents may depend on semantic content, relying solely on spatial and class information can introduce errors. Our method can encode text content into embeddings and add them with positional embeddings to incorporate semantic cues, which yields an approximate 0.13% performance improvement on OmniDocBench v1.5, albeit at the cost of increased computational overhead. Nonetheless, our method may still suffer from errors in layout detection, which can propagate to subsequent recognition steps. For example, directly detecting rectangular boxes may be inaccurate for photographed documents, and handling complex layouts that require semantic understanding may remain insufficient. Challenges such as cross-page tables and paragraphs, hierarchical headings, and multi-page document parsing also persist.

## G. Comparison with other Methods

We further compare our method with the state-of-the-art pipeline approaches, MinerU2-Pipeline [49] and PPStruct-V3 [9], with results shown in Fig. 9. The visualizations indicate that these pipeline methods often produce unnecessary superscripts and incorrect symbols when recognizing inline formulas. This issue primarily arises from inaccuracies in inline formula detection, which lead to error accumulation across multiple processing stages. In contrast, our method simplifies the pipeline by directly feeding the text block into an LMM for recognition, resulting in stronger robustness and more accurate outputs.

We compared MonkeyOCR-3B with Qwen2.5VL-7B [1] and InternVL3.5-8B [6], with results shown in Fig. 10. Despite having fewer parameters, MonkeyOCR-3B accurately reconstructs both the structure and content of the table. In contrast, Qwen2.5VL-7B exhibits errors in table structure recognition, while InternVL3.5-8B not only misidentifies table structures but also makes mistakes in symbol recognition. These results demonstrate that MonkeyOCR-3B excels in table recognition, benefiting from the abundant table recognition samples in the MonkeyDoc dataset.

## (a) Image

mechanisms when solving multimodal tasks.

**Mechanistic interpretability of MLLMs** Mechanistic interpretability [31, 33] is an emerging research area in NLP, aiming to reverse-engineer detailed computations within neural networks. While it has gained attraction in NLP, research in the multimodal domain remains limited. Palit et al. [34] introduced a causal tracing tool for image-conditioned text generation on BLIP [23], marking one of the few early efforts in this area. Several initial studies have started to explore the internal states of MLLMs by linking external behaviours to specific mechanisms, such as information storage in model parameters [6], undesirable content generation reflected in the logit distributions of the first generated token [46], localization and evolution of object-related visual information [32, 34, 37], safety mechanism localization [43], and reducing redundant visual tokens [45]. However, research offering a comprehensive understanding of the internal mechanisms behind multimodal information integration in MLLMs is still lacking. This paper makes an important first step towards filling this gap.

### 3. Tracing information flow in MLLMs

The focus of this paper is on auto-regressive multimodal large language models, which consist of an image encoder and a decoder-only language model, as shown in Figure 2. The image encoder transforms images into representations that the language model can take as input, while the language model integrates these visual cues with any provided text, generating responses one word at a time. Often, these components are initialized from a pre-trained image encoder (e.g. CLIP-ViT-336px [33]) and a large language model (e.g. Llama2 [40]) respectively. Since the interaction between modalities only occurs in the decoder-only transformer, our analysis centers around it and we refer to it as MLLM for brevity unless otherwise specified.

#### 3.1. Background: MLLMs

**Input** The input to an MLLM typically comprises image and text features, with the image features being initially extracted from an image encoder and the text being encoded through word embeddings. Formally, an image  $x$  is evenly split into fixed-size patches and encoded by an image encoder to obtain  $N_V$  visual patch features  $V = [v_1]_{i=1}^{N_V}, v_i \in \mathbb{R}^d$ . Similarly, the text  $t$ , consisting of  $N_T$  tokens, is embedded into representations through a lookup table of word embeddings, resulting in the text input  $T = [t_i]_{i=1}^{N_T}, t_i \in \mathbb{R}^d$ . By concatenation of  $V$  and  $T$ , the multimodal input sequence  $I = [v_1 \dots v_{N_V}, t_1 \dots t_{N_T}] \in \mathbb{R}^{N \times d}$ , where  $N = N_V + N_T$ , is fed into MLLM.

**Hidden representation** The input sequence is fed into the MLLM, where the hidden representation at each token position is encoded across  $L$  transformer layers. Each layer primarily

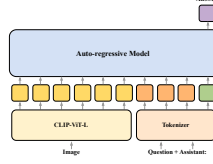


Figure 2. The typical architecture of multimodal large language model. It consists of an image encoder and a decoder-only large language model in which the multimodal information is integrated. We omitted the projection matrix for the visual patch feature as it is nonessential for our analysis.

consists of two modules: a masked multi-head attention (MHAT) followed by a fully connected feed-forward network (FFN) [41]. For conciseness, we have excluded the bias terms and layer normalization, as they are not crucial for our analysis. Formally, the hidden representation  $h_i^\ell \in \mathbb{R}^d$  in the position  $i$  of the input sequence at layer  $\ell$  can be expressed as

$$h_i^\ell = h_i^{\ell-1} + a_i^\ell + f_i^\ell, \quad (1)$$

where  $a_i^\ell \in \mathbb{R}^d$  and  $f_i^\ell \in \mathbb{R}^d$  are the outputs of MHAT and FFN modules at layer  $\ell$ , respectively.  $h_i^\ell$  represents a vector in the input  $I$  with position of  $i$ . All hidden representations at layer  $\ell$  corresponding to the whole input  $I$  can be denoted by  $\hat{H}^\ell = [h_i^\ell]_{i=1}^N \in \mathbb{R}^{N \times d}$ .

**MHAT** The masked multi-head attention (MHAT) module in each transformer layer  $\ell$  contains four projection matrices:  $W_Q^\ell, W_K^\ell, W_V^\ell, W_O^\ell \in \mathbb{R}^{d \times d}$ . For the multi-head attention, the input  $H^{\ell-1}$  is first projected to query, key and value:  $Q^\ell = H^{\ell-1}W_Q^\ell, K^\ell = H^{\ell-1}W_K^\ell, V^\ell = H^{\ell-1}W_V^\ell$ . Then the projected query, key and value matrices are evenly split along the columns to  $H$  different heads:  $\{Q^{i,j}\}_{j=1}^H, \{K^{i,j}\}_{j=1}^H, \{V^{i,j}\}_{j=1}^H \in \mathbb{R}^{d \times \frac{d}{H}}$ , respectively. After splitting  $W_O^\ell$  into  $\{W_O^{i,j}\}_{j=1}^H \in \mathbb{R}^{d \times \frac{d}{H}}$ , we follow works in [12, 15, 19] to represent the output of MHAT  $A^\ell = [a_i^\ell]_{i=1}^N \in \mathbb{R}^{N \times d}$  at layer  $\ell$  as the sum of the output from different heads

$$A^\ell = \sum_{j=1}^H A^{\ell,j} V^{\ell,j} W_O^{\ell,j} \quad (2)$$

$$A^{\ell,j} = \text{softmax} \left( \frac{Q^{i,j} (K^{i,j})^T}{\sqrt{d/H}} + M^{\ell,j} \right) \quad (3)$$

## (c) PPStruct-V3

mechanisms when solving multimodal tasks.

**Input** The input to an MLLM typically comprises image and text features, with the image features being initially extracted from an image encoder and the text being encoded through word embeddings. Formally, an image  $x$  is evenly split into fixed-size patches and encoded by an image encoder to obtain  $N_V$  visual patch features  $\hat{V} = [\hat{v}_i]_{i=1}^{N_V}, v_i \in \mathbb{R}^d$ .

where  $a_i^\ell \in \mathbb{R}^d$  and  $f_i^\ell \in \mathbb{R}^d$  are the outputs of MHAT and FFN modules at layer  $\ell$ , respectively.  $h_i^\ell$  represents a vector in the input  $I$  with position of  $i$ . All hidden representations at layer  $\ell$  corresponding to the whole input  $I$  can be denoted by  $\hat{H}^\ell = [h_i^\ell]_{i=1}^N \in \mathbb{R}^{N \times d}$

**MHAT** The masked multi-head attention (MHAT) module in each transformer layer contains four projection matrices:  $W_Q^\ell, W_K^\ell, W_V^\ell, W_O^\ell \in \mathbb{R}^{d \times d}$ . For the multi-head attention, the input  $H^{\ell-1}$  is first projected to query, key and value:  $Q^\ell = H^{\ell-1}W_Q^\ell, K^\ell = H^{\ell-1}W_K^\ell, V^\ell = H^{\ell-1}W_V^\ell$ . Then the projected query, key and value matrices are evenly split along the columns to  $H$  different heads:  $\{Q^{i,j}\}_{j=1}^H, \{K^{i,j}\}_{j=1}^H, \{V^{i,j}\}_{j=1}^H \in \mathbb{R}^{N \times \frac{d}{H}}$ , respectively.

## (b) MonkeyOCR

mechanisms when solving multimodal tasks.

### 3.1. Background: MLLMs

**Input** The input to an MLLM typically comprises image and text features, with the image features being initially extracted from an image encoder and the text being encoded through word embeddings. Formally, an image  $x$  is evenly split into fixed-size patches and encoded by an image encoder to obtain  $N_V$  visual patch features  $V = [v_i]_{i=1}^{N_V}, v_i \in \mathbb{R}^d$ . Similarly, the text  $t$ , consisting of  $N_T$  tokens, is embedded into representations through a lookup table of word embeddings, resulting in the text input  $T = [t_i]_{i=1}^{N_T}, t_i \in \mathbb{R}^d$ . By concatenation of  $V$  and  $T$ , the multimodal input sequence  $I = [v_1 \dots v_{N_V}, t_1 \dots t_{N_T}] \in \mathbb{R}^{N \times d}$ , where  $N = N_V + N_T$ , is fed into MLLM.

For conciseness, we have excluded the bias terms and layer normalization, as they are not crucial for our analysis. Formally, the hidden representation  $h_i^\ell \in \mathbb{R}^d$  in the position  $i$  of the input sequence at layer  $\ell$  can be expressed as

$$h_i^\ell = h_i^{\ell-1} + a_i^\ell + f_i^\ell,$$

where  $a_i^\ell \in \mathbb{R}^d$  and  $f_i^\ell \in \mathbb{R}^d$  are the outputs of MHAT and FFN modules at layer  $\ell$ , respectively.  $h_i^\ell$  represents a vector in the input  $I$  with position of  $i$ . All hidden representations at layer  $\ell$  corresponding to the whole input  $I$  can be denoted by  $\hat{H}^\ell = [h_i^\ell]_{i=1}^N \in \mathbb{R}^{N \times d}$ . MHAT The masked multi-head attention (MHAT) module in each transformer layer  $\ell$  contains four projection matrices:  $W_Q^\ell, W_K^\ell, W_V^\ell, W_O^\ell \in \mathbb{R}^{d \times d}$ . For the multi-head attention, the input  $H^{\ell-1}$  is first projected to query, key and value:  $Q^\ell = H^{\ell-1}W_Q^\ell, K^\ell = H^{\ell-1}W_K^\ell, V^\ell = H^{\ell-1}W_V^\ell$ . Then the projected query, key and value matrices are evenly split along the columns to  $H$  different heads:  $\{Q^{i,j}\}_{j=1}^H, \{K^{i,j}\}_{j=1}^H, \{V^{i,j}\}_{j=1}^H \in \mathbb{R}^{N \times \frac{d}{H}}$ , respectively. After splitting  $W_O^\ell$  into  $\{W_O^{i,j}\}_{j=1}^H \in \mathbb{R}^{d \times \frac{d}{H}}$ , we follow works in [12, 15, 19] to represent the output of MHAT  $A^\ell = [a_i^\ell]_{i=1}^N \in \mathbb{R}^{N \times d}$  at layer  $\ell$  as the sum of the output from different heads

$$A^\ell = \sum_{j=1}^H A^{\ell,j} V^{\ell,j} W_O^{\ell,j}$$

$$A^{\ell,j} = \text{softmax} \left( \frac{Q^{i,j} (K^{i,j})^T}{\sqrt{d/H}} + M^{\ell,j} \right)$$

## (d) MinerU2-Pipeline

mechanisms when solving multimodal tasks.

through word embeddings. Formally, an image  $x$  is evenly split into fixed-size patches and encoded by an image encoder to obtain  $N_V$  visual patch features  $V = [\hat{v}_i]_{i=1}^{N_V}, v_i \in \mathbb{R}^d$ . Similarly, the text  $t$ , consisting of  $N_T$  tokens, is embedded into representations through a low-rank embeddings, resulting in the text input  $T = [t_i]_{i=1}^{N_T}$ . By concatenation of and , the multimodal input sequence  $I = [v_1 \dots v_{N_V}, t_1 \dots t_{N_T}] \in \mathbb{R}^{N \times d}$ , where  $N = N_V + N_T$ , is fed into MLLM.

respectively.  $h_i^\ell$  represents a vector in the input  $I$  with position of  $i$ . All hidden representations at layer  $\ell$  corresponding to the whole input  $I$  can be denoted by  $\hat{H}^\ell = [h_i^\ell]_{i=1}^N \in \mathbb{R}^{N \times d}$ . MHAT The masked multi-head attention (MHAT) module in each transformer layer  $\ell$  contains four projection matrices:  $W_Q^\ell, W_K^\ell, W_V^\ell, W_O^\ell$ . For the multi-head attention, the input  $H^{\ell-1}$  is first projected to query, key and value:  $Q^\ell = H^{\ell-1}W_Q^\ell, K^\ell = H^{\ell-1}W_K^\ell, V^\ell = H^{\ell-1}W_V^\ell$ . Then the projected query, key and value matrices are evenly split along the columns to  $H$  different heads:  $\{Q^{i,j}\}_{j=1}^H, \{K^{i,j}\}_{j=1}^H, \{V^{i,j}\}_{j=1}^H \in \mathbb{R}^{N \times \frac{d}{H}}$ , respectively.

Figure 9. Visual comparison with pipeline methods, with errors highlighted in red.

(a) Image

**最新部编版六年级语文下册教材目录**  
部编版六年级下册教材目录（送审版）

六下	第一单元	1. 北京的春节 2. 腊八粥 3. 古诗三首 寒食/（唐）韩翃 迢迢牵牛星/《古诗十九首》 十五夜望月/（唐）王建 4*. 藏戏 习作：家乡的风俗 语文园地一 游子吟/（唐）孟郊
	第二单元	5. 鲁滨孙漂流记（梗概+节选） 6*. 骑鹅旅行记（节选） 7*. 汤姆·索亚历险记 口语交际：同读一本书 习作：写作品梗概 语文园地二 快乐读书吧：漫步世界名著花园
	第三单元	8. 匆匆 9. 那个星期天 习作例文： 别了，国语课 小桥流水人家 习作：让真情自然流露 语文园地三 《天净沙·秋思》（元）马致远
	第四单元	过零丁洋（宋）文天祥 10. 古诗三首 马诗/（唐）李贺 石灰吟/（明）于谦 竹石/（清）郑 11. 十六年前的回忆

(b) MonkeyOCR

**最新部编版六年级语文下册教材目录**  
部编版六年级下册教材目录（送审版）

六下	第一单元	1. 北京的春节 2. 腊八粥 3. 古诗三首 寒食/（唐）韩翃 迢迢牵牛星/《古 诗十九首》 十五夜望月/（唐）王 建 4*. 藏戏 习作：家乡的风俗 语 文园地一 游子吟/（唐）孟郊
	第二单元	5. 鲁滨孙漂流记（梗概+节选） 6*. 骑鹅旅行记（节选） 7*. 汤姆· 索亚历险记 口语交际：同读一本 书 习作：写作品梗概 语文园地二 快乐读书吧：漫步世界名著花园
	第三单元	8. 匆匆 9. 那个星期天 习作例文： 别了，国语课 小桥流水人家 习作： 让真情自然流露 语文园地三 《天 净沙·秋思》（元）马致远
	第四单元	过零丁洋（宋）文天祥 10. 古诗三 首 马诗/（唐）李贺 石灰吟/（明） 于谦 竹石/（清）郑 11. 十六年前 的回忆

(c) Qwen2.5VL-7B

**最新部编版六年级语文下册教材目录**  
部编版六年级下册教材目录（送审版）

六下	第一单元	1. 北京的春节 2. 腊八粥 3. 古诗三 首 寒食/（唐）韩翃 迢迢牵牛星/ 《古诗十九首》 十五夜望月/（唐 王建 4*. 藏戏 习作：家乡的风俗 语文园地一 游子吟/（唐）孟郊
	第二单元	5. 鲁滨孙漂流记（梗概+节选） 6*. 骑鹅旅行记（节选） 7*. 汤 姆·索亚历险记 口语交际：同读一 本书 习作：写作品梗概 语文园地 二 快乐读书吧：漫步世界名著花 园
	第三单元	8. 匆匆 9. 那个星期天 习作例文： 别了，国语课 小桥流水人家 习作： 让真情自然流露 语文园地三 《天净沙·秋思》（元）马致远
	第四单元	过零丁洋（宋）文天祥 10. 古诗 三首 马诗/（唐）李贺 石灰吟/ （明）于谦 竹石/（清）郑 11. 十 六年前的回忆

(d) InternVL3.5-8B

**最新部编版六年级语文下册教材目录**

部编版六年级下册教材目录（送审版）

六下	第一单元
	1. 北京的春节
	2. 腊八粥
	3. 古诗三首
	寒食/（唐）韩翃
	迢迢牵牛星/《古诗十九首》
	十五夜望月/（唐）王建
	4*. 藏戏
	习作：家乡的风俗
	语文园地一
	游子吟/（唐）孟郊

六下	第二单元
	5. 鲁滨孙漂流记
	（梗概+节选）
	6*. 骑鹅旅行记（节选）
	7*. 汤姆·索亚历险记
	口语交际：同读一本书
	习作：写作品梗概
	语文园地二
	快乐读书吧：漫步世界名著花园

六下	第三单元
	8. 勇敢
	9. 那个星期天
	习作例文：
	别了，国语课
	小桥流水人家
	习作：写作品梗概
	语文园地三
	《天净沙·秋思》（元）马致远

六下	第四单元
	过零丁洋（宋）文天祥
	10. 古诗三首
	马诗/（唐）李贺
	石灰吟/（明）于谦
	竹石/（清）郑
	11. 十六年前的回忆

Figure 10. Visual comparison with end-to-end models, with errors highlighted in red.